

# SDSS J1130+0058 an X-shaped Radio Source With Double-Peaked Low-Ionization Emission Lines: A binary Black Hole System?

Xue-Guang Zhang<sup>1\*</sup>, Dultzin-Hacyan D.<sup>1</sup>, Ting-Gui Wang<sup>2</sup>

<sup>1</sup>*Instituto de Astronomia, Universidad Nacional Autonoma de Mexico, Apdo Postal 70-264, Mexico D. F. 04510, Mexico*

<sup>2</sup>*Center for Astrophysics, Department of astronomy and Applied Physics, University of Science and Technology of China, Hefei, Anhui, P.R. China*

## ABSTRACT

In this paper we study the object SDSS J1130+0058 which is the only AGN known to have both double-peaked low-ionization broad emission lines, and also X-shaped radio structures. Emission from an accretion disk can reproduce the double-peaked line profile of broad H $\alpha$ , but not the radio structure. Under the accretion disk model, the period of the inner emission line region is about 230 years. Using a new method to subtract the stellar component from the data of the SDSS DR4, we obtain an internal reddening factor which is less than previously found. The implied smaller amount of dust disfavors the backflow model for the X-shaped radio structure. The presence of a Binary Black Hole (BBH) system is the most natural way to explain *both* the optical and radio properties of this AGN. Under the assumption of the BBH model, we can estimate the BBH system has a separation of less than 0.04 pc with a period less than 59 years, this may pose some problem to the BLRs sizes, still we conclude that the BBH model is favored on the basis of the present limited information.

**Key words:** Galaxies:Active – galaxies:nuclei – galaxies:jets – accretion,accretion disks – black hole physics

## 1 INTRODUCTION

The detailed structure of the inner parts of Active Galactic Nuclei (AGN): the black hole, accretion disk and broad emission line regions (BLRs), cannot be resolved by direct observations, with the possible exception of indirect evidence from a dusty torus in the nucleus of NGC4261. The use of reverberation mapping (Peterson 1993; Netzer & Peterson 1997; Blandford & McKee 1982) requires the assumption of a rough geometric structure for the BLRs in order to explain the correlation between the variations of broad emission lines and those of continuum. Moreover, the problem of spatially resolving these regions, will not be solved in the foreseeable future. Up until now, the best approach is the detailed study of broad line profile shapes and asymmetries from high S/N spectra (Sulentic et al. 2000; Marziani, Dultzin-Hacyan & Sulentic 2006).

There are at least three special types of AGN where the observed phenomenology has suggested the presence of a binary black hole system (BBH) in the center: (1) blazars with periodical brightness variations, (2) AGN with X-shaped

radio structures (X-shaped AGN), and (3) double-peaked broad low-ionization line (dbl) emitters.

In the prototypical case of the periodically varying blazar OJ 287 (Sillanpää et al. 1996a, 1996b; Valtonen et al. 2006a) the bending of the VLBI (Very Long Baseline Interferometry) jet was first reported by Vicente et al. (1996). A very small change in the orientation of the jet is needed to change the Doppler boosting dramatically, thereby producing long-term periodic brightness modulations. Sillanpää et al. (1988) and Lehto & Valtonen (1996) modeled the periodic outbursts by relating them to tidally induced mass flows from the accretion disks in a BBH system with an orbital period of 8.9 years (in the rest frame of OJ 287). The predictions of the model have been confirmed quite spectacularly (Valtonen et al. 2006a; Valtonen et al. 2006b).

The first and most famous dbl emitters are NGC 1097 (Storchi-Bergmann, Nemmen, et al. 2003; Storchi-Bergmann, Eracleous et al. 1997; Storchi-Bergmann, Eracleous & Halpern 1995; Storchi-Bergmann, Baldwin et al. 1993), Arp102B (Chen et al. 1989, 1997; Chen & Halpern 1989; Halpern et al. 1996; Antonucci et al. 1996; Sulentic et al. 1990) and 3C390.3 (Shapovalova et al. 2001; Gilbert et al. 1999). The first natural explanation for the appearance of double peaked emission lines was also a BBH model (Begel-

\* xguang@astroscu.unam.mx

man et al. 1980; Gaskell 1983). Another model of bipolar outflow was proposed by Zheng et al. (1990). The most successful model involved lines originating from an accretion disk to explain not only the appearance, but also the observed variations of double-peaked emission lines (Chen et al. 1989; Chen & Halpern 1989). The simple accretion disk model has been modified to better fit the observations to an elliptical disk by Eracleous et al. (1995), to a warped accretion disk by Bachev (1999) and Hartnoll & Blackman (2000), and to a circular accretion disk plus spiral arms by Chakrabarti & Wiita (1994), Hartnoll & Blackman (2002) and Karas, Martocchia & Subr (2001). An important reason to give up the initial BBH model was the unreasonable BH masses derived from the variations of the broad emission lines for three dbp emitters (Eracleous et al. 1997). In the case of the bipolar outflow model, the observed variations could not be explained.

Another special kind of AGN, X-shaped AGN, are classified according to their extended radio morphology. One of the first explanations for the distortion of radio structures, particularly for X-shaped and Z-shaped AGN, was backflow material dominating the bridge regions (Leahy & Williams 1984; Worrall et al. 1995). More recently, other models have also been developed to explain the distortions, such as the precession of jet axis in a BBH system. It should be noticed that in the case of OJ287 (the first confirmed periodically varying blazar), the bending of the VLBI jet was first reported by Vicente et al. (1996). Objects with bending, misalignment, and wiggling of extragalactic radio jets (often associated with knots superluminally moving along different-scale curved trajectory), have been interpreted in terms of helical structures of the jets. This structure is likely caused by the precession of the jet in a binary black hole system (both kinds of models are discussed in e.g.: Dennett-Thorpe et al. 2002; Merritt & Ekers 2002; Liu 2004; Caproni & Abraham 2004a, 2004b; Ostorero, Villata & Raiteri 2004). Up to the present, there are more than ten X-shaped AGN reported in the literature.

It seems only natural to invoke a BBH system to explain the presence of both dbp lines and X-shaped jets in an AGN. In this paper, we report the only such object so far known: SDSS J113021.41+005823 (hereafter, SDSS J1130+0058, found in SDSS DR4 (York et al. 2000; Strauss et al. 2002; Abazajian et al. 2004; Berk et al. 2001; Scott et al. 2004)). The next section presents the observational data. In Section 3 we present the discussion and conclusions. In this paper, the cosmological parameters  $H_0 = 70 \text{ km} \cdot \text{s}^{-1} \text{Mpc}^{-1}$ ,  $\Omega_\Lambda = 0.7$  and  $\Omega_m = 0.3$  have been adopted.

## 2 OBSERVED RESULTS

### 2.1 Results at Optical Band

SDSS J1130+0058 has been studied by Wang et al. (2003) with another target name (4C +01.30), as an obscured quasar. Thus, in this section, we briefly discuss the observed results at optical band. The apparent optical Petrosian magnitudes of SDSS J1130+0058 ( $z = 0.13$ ) are 18.43, 17.13, 16.19, 15.72, 15.49 at u, g, r, i and z bands, respectively. The galactic reddening corrected (with  $E(B-V) = 0.022$ ) spectrum of SDSS J1130+0058 with total exposure time of 3600 seconds is shown in Figure 1.

In order to measure the line parameters more accurately, the component due to the host galaxy must be removed from the observed spectrum. We believe that the most convenient way to subtract this component is the PCA (Principle Component analysis) method described by Li et al. (2005) and Hao et al. (2005), using the eigenspectra from pure absorption galaxies from SDSS or the eigenspectra from stars in STELIB (Le Borgne et al. 2003). Here, we used the method from Hao et al. (2005). The eigenspectra are calculated by KL (Karhunen-Loeve) transform for about 926 pure absorption galaxies selected from SDSS DR2. Then, the first eight eigenspectra and the spectrum of an A star are used to fit the absorption properties of the observed spectrum. A power law is used to fit the continuum from the nuclei. The line spectrum of SDSS J1130+0058, after the subtraction of the stellar component and power law continuum, are show in Figure 2. The stellar components and the power law continuum are also shown in the figure. The best fitted results for absorption lines, such as the CaII $\lambda\lambda 3934, 3974 \text{\AA}$  doublet, indicate that the subtraction of stellar components is reliable. As discussed in Wang et al. (2003), there is apparent broad H $\alpha$  emission line and weak broad H $\beta$  emission line in line spectrum.

After the subtraction of the stellar light and continuum, the emission line parameters are measured. The line parameters were listed in Wang et al. (2003), however, new eigenspectra and new observed spectrum from SDSS DR4 are used here, thus, we re-measured the emission lines and list our new line parameters in Table 1. We fit each narrow emission line by a narrow gaussian function. For [OIII] $\lambda\lambda 4959, 5007 \text{\AA}$  doublet, there are other two gaussian functions for each line, because of the asymmetry of [OIII] $\lambda\lambda 4959, 5007 \text{\AA}$ . Due to the weakness of broad H $\beta$ , we use the broad component of H $\alpha$  to fit broad H $\beta$ . First, we obtain the broad component of H $\alpha$  after the subtraction of narrow H $\alpha$ , [NII] $\lambda\lambda 6548, 6583 \text{\AA}$  and [SII] $\lambda\lambda 6716, 6731 \text{\AA}$  within the wavelength range from  $6400 \text{\AA}$  to  $6800 \text{\AA}$ . In order to get more accurate narrow components near H $\alpha$ , there are two broad gaussian functions to fit the broad H $\alpha$ . Then the narrow components near H $\alpha$  according to the best fitted results are subtracted from the observed line spectrum. We have assumed that broad H $\beta$  and H $\alpha$  have the same line profiles, thus we can estimate the flux ratio of broad H $\alpha$  to H $\beta$ . The best fitted results for H $\alpha$  are shown in Figure 3. Figure 4 shows the best fitted results for H $\beta$  by scaling of the observed broad H $\alpha$ .

The object SDSS J1130+0058, has been considered as a dbp emitter in the sample of dbp emitters by Strateva et al. (2003). In our new sample of dbp emitters (Zhang et al. in preparation) from SDSS DR4, this object also is a dbp emitter. For preliminary definition of criteria see also Zhang, Dultzin-Hacyan & Wang (2007).

### 2.2 Results at Radio Band

The radio image at 20cm for SDSS J1130+0058 can be extracted from Faint Images of the Radio Sky at Twenty centimeter Survey (FIRST, Becker, White & Helfand 1995), which is shown in Figure 5. The apparent X-shaped radio morphology can be seen. There are four regions which strongly emit radio power as listed in Table 2. As discussed in Wang et al. (2003), the smallest offset of the photometric

center from the four radio regions is about 4.5 arcseconds which is larger than the position uncertainty of SDSS and FIRST, which indicates that the central component may be a component from the jet rather than the radio core. The total integral radio power at 20cm for SDSS J1130+0058 is about  $10^{25.42} \text{W} \cdot \text{Hz}^{-1}$ .

Furthermore, one fundamental parameter of a radio jet, the age of the jet, is important to understand the physical processes in the forming the jet. There are many papers that discuss the age of a jet, including the dynamical and spectral age. Alexander & Leahy (1987) firstly proposed the method to measure the spectral age of a radio jet (the same methods can be found in Leahy et al. 1989; Liu et al. 1992; Parma et al. 1999). Spectral age depends on the break frequency  $\mu_{br}$ , which can be calculated by the spectral index at different frequencies in various regions. The more accurate dynamical age is more difficult to calculate and depends on the model of dynamical expansion (Kaiser & Alexander 1997; Kaiser 2000; Kaiser et al. 1997; Parma et al. 1999; Machalski et al. 2006; Tudose et al. 2006; Kino & Kawakatu 2005). The limit on the radio data is not enough to calculate the accurate age. However, we can determine which one is older. Machalski et al. (2006) have found there is a strong linear correlation between spectral age and dynamical age (dynamical age is about two times the spectral age). The spectral age  $t_s$  can simply depend on the distance between the lobe edge and the core  $x$ :  $t_s \propto x$ , considering the relation between  $x$  and  $\mu_{br}$  shown in Parma et al. (1999). Thus as a simple empirical result, we can say that the double-jet in the N-S direction is older than the one in E-W direction, because of the longer projected distance in N-S direction.

### 3 DISCUSSIONS AND CONCLUSIONS

#### 3.1 An obscured AGN?

The internal reddening factor can be determined by the value of the Balmer decrement. The flux ratios of the Balmer emission lines are about 3.78 and 6.52 for the narrow and broad components respectively. It should be pointed out, however, that the intrinsic Balmer decrement is not a definitive value for AGN, because case B recombination is not necessarily valid (particularly for the BLR). The value of 3.1 can be expected by Case B recombination. From a sample of quasars with smaller contribution from the host galaxy, the mean value is about 3.5 (Greene & Ho, 2005b). If we assume the intrinsic Balmer decrement as 3.1, the internal reddening factors are about  $E(B-V)=0.64$  for the broad Balmer emission lines, and  $E(B-V) = 0.17$  for the narrow Balmer emission lines. The Balmer decrement is not as large as the one determined by Wang et al. (2003).

In order to verify if the internal reddening factor leads to luminosities which agree with well established scaling relations, we have used the tight correlation between continuum luminosity at 5100Å and the luminosity of H $\alpha$  found by Greene & Ho (2005b). The observed luminosity of H $\alpha$  including the narrow component of H $\alpha$  is about  $1.16 \times 10^{42} \text{erg} \cdot \text{s}^{-1}$  ( $9.08 \times 10^{41} \text{erg} \cdot \text{s}^{-1}$  for broad component and  $2.47 \times 10^{41} \text{erg} \cdot \text{s}^{-1}$  for narrow component). The continuum luminosity at 5100Å from the nucleus can be measured from the power law continuum,  $L_{5100\text{\AA}} = 1.09 \times$

$10^{43} \text{erg} \cdot \text{s}^{-1}$ . The total continuum luminosity at 5100Å from the observed spectrum is approximately  $4.79 \times 10^{43} \text{erg} \cdot \text{s}^{-1}$ . After the internal reddening correction with  $E(B-V) = 0.64$ , the intrinsic continuum luminosity at 5100Å from the nucleus is about  $8.03 \times 10^{43} \text{erg} \cdot \text{s}^{-1}$ , and the intrinsic luminosity  $L_{H\alpha}$  is about  $4.01 \times 10^{42} \text{erg} \cdot \text{s}^{-1}$  (the luminosity of narrow H $\alpha$  has been corrected by the factor  $E(B-V)=0.17$ ). The relation between the corrected values are consistent with the expectation from the correlation found by Greene & Ho (2005b):

$$L_{H\alpha} = 5.25 \times 10^{42} \left( \frac{L_{5100\text{\AA}}}{10^{44} \text{erg} \cdot \text{s}^{-1}} \right)^{1.157} \text{erg} \cdot \text{s}^{-1} \quad (1)$$

This consistency confirms that the method of subtracting stellar components is valid and the calculated internal reddening factor is a reasonable estimate. SDSS J1130+0058 is indeed an obscured AGN with intermediate internal reddening. The smaller value for internal reddening found in this paper (as compared to Wang et al. 2003) implies a smaller amount of internal dust, and thus a lower density for the internal regions. However, the backflow model requires a higher gas pressure in the direction of the galaxy, as shown in other X-shaped radio sources there are nearly no detectable broad emission lines because of the higher internal reddening. This does not favor the backflow model for the X-shaped radio structure in SDSS J1130+0058.

#### 3.2 BH Masses and Accretion Rate

There are mainly two methods to estimated the central BH masses: One is from the correlation between the masses of the bulge and the central Black Hole following the strong correlation between BH masses and stellar velocity dispersion (Tremaine et al. 2002; Ferrarese & Merritt 2001; Gebhardt, Bender et al. 2000) (or line width of narrow emission lines, Greene & Ho 2005a; Nelson & Whittle 1995, 1996; Nelson 2000), and the correlation between absolute magnitude of the bulge and BH masses (Kormendy & Gebhardt 2001) etc. The other one is from the assumption of virialization (Kaspi et al. 2000; Peterson & Wandel 1999; Peterson et al. 2004; Onken et al. 2004; Sulentic et al. 2006), based on the line width of broad emission lines and the size of broad emission line regions estimated from continuum luminosity (Kaspi et al. 2000; 2005). As shown in Kazantzidis et al. (2005), the central masses of merging galaxies should also obey the strong correlation between BH masses and stellar velocity dispersions, if they undergo a dissipational process with star formation mergers. Moreover, according to the hierarchical merging model, we think the BBH system is common in the center of AGN. Even in the sample used to obtain the strong relation  $M_{BH} - \sigma$  (Tremaine et al. 2002; Ferrarese & Merritt 2001; Gebhardt, Bender et al. 2000), we cannot discard the possibility that the centers of the objects have BBH system. Thus, whether there is a BBH system in the center of SDSS J1130+0058 or not, we estimate the BH masses from stellar velocity dispersions.

How to measure accurately stellar velocity dispersions is an open question, because of the known problem about the template mismatch. A commonly used method is to select spectra of several kinds of stars (commonly, G and K) as templates, and then broaden the templates by the

same velocity to fit stellar features, leaving the contributions from different kinds of stars as free parameters (Rix & Whit 1992). However, more information about stars included by the templates should lead to more accurate measurement of stellar features. According to the above mentioned fitting method, we selected a new template rather than several spectra of G or K stars as templates. The method of Principle Component Analysis (PCA) provides a better way to constrict more favorable information from a series of spectra of stars into several eigenspectra. Thus, we apply PCA method for 255 spectra of different kinds of stars in STELIB. Selecting the first several eigenspectra and a three-order polynomial function for the background as templates, the value of the stellar velocity dispersion can be measured by means of the method of minimum  $\chi^2$  fit. Figure 6 shows the fitted results for the stellar features near  $\text{MgI}\lambda 5175\text{\AA}$  by means of the eigenspectra with broadening velocity  $\sigma = 142.6 \pm 22.6 \text{ km} \cdot \text{s}^{-1}$ . The error in the stellar velocity dispersion is determined from the different numbers of required eigenspectra. Here, 4 to 8 eigenspectra are used to fit the stellar features. The central BH masses of SDSS J1130+0058 can be estimated as  $M_{BH} = 3.83_{-2.37}^{+4.44} \times 10^7 \text{ M}_\odot$  by (Tremaine et al. 2002; Ferrarese & Merritt 2001; Gebhardt, Bender et al. 2000):

$$M_{BH} = 10^{8.13 \pm 0.06} \left( \frac{\sigma}{200 \text{ km} \cdot \text{s}^{-1}} \right)^{4.02 \pm 0.32} \text{M}_\odot \quad (2)$$

Moreover, we should select another parameter to estimate the central BH masses. The convenient way is to select the line width of narrow emission lines to trace the stellar velocity dispersion in the bulge. From the line widths of narrow emission lines listed in Table 1, the minimum value of line width ( $\sigma_{line}$ ) is  $103.3 \text{ km} \cdot \text{s}^{-1}$  for  $\text{H}\delta$  and the maximum value is  $175.6 \text{ km} \cdot \text{s}^{-1}$  for  $[\text{OII}]\lambda 3727\text{\AA}$ . Thus, we can estimated the BH masses as  $9.47 \times 10^6 - 8.01 \times 10^7 \text{ M}_\odot$  by the relation of  $M_{BH} - \sigma$ , which is consistent with the value from stellar velocity dispersion and confirms the strong correlation between stellar velocity dispersion and line width of narrow emission lines.

The virial BH masses are based on the empirical relation between the size of BLRs and continuum luminosity. However, the broad emission lines of SDSS J1130+0058 have special double-peaked profiles. Thus, either under the accretion disk model or under the BBH model, the size of BLRs of the object should not obey the empirical relation  $R_{BLRs} - L_{5100\text{\AA}}$ .

For accretion rate, we can determine the dimensionless accretion rate based on the bolometric luminosity and Eddington luminosity to trace the accretion rate. The bolometric luminosity for AGN with normal spectral energy distribution, such as normal big blue bump, can be determined by the continuum luminosity  $L_{bol} \sim 9 \times L_{5100\text{\AA}}$ . The Eddington luminosity can be determined by  $L_{Edd} \sim 1.38 \times 10^{38} M_{BH} / \text{M}_\odot \text{ erg} \cdot \text{s}^{-1}$ . Thus, the dimensionless accretion rate can be determined as  $\dot{m} \sim L_{bol} / L_{Edd} \sim 0.06 - 0.36$ , which is larger than the critical accretion rate for ADAF (Mahadevan & Quataert 1997; Narayan et al. 1995, 1996; Mahadevan 1997).

### 3.3 Accretion Disk Model or BBH model for double-peaked $\text{H}\alpha$ ?

First, we check whether the BBH model can be valid for SDSS J1130+0058. From the best fitted results shown in Figure 3, double-gaussian functions can completely reproduce the observed double-peaked broad  $\text{H}\alpha$ . If the BBH model is valid, the observed radial velocity of each peak of each broad component of  $\text{H}\alpha$  represents the rotating velocity in the line of sight,  $v_1 \sim 1065 \text{ km} \cdot \text{s}^{-1}$  and  $v_2 \sim -2354 \text{ km} \cdot \text{s}^{-1}$ . Here, the minus means the component is moving toward us. Then the mass ratio of the two central BH masses can be roughly determined by  $M_{BH1}/M_{BH2} \sim v_2/v_1 \sim 2.2$ , if the separation between the central two black holes is much larger than the distance between BLRs and each corresponding black hole. Here,  $M_{BH1}$  represents the black hole with larger BH mass. However, whether the relation  $M_{BH} - \sigma$  is valid for merging galaxies depends on whether the merger is dissipative or colisionless (Kazantzidis et al. 2005). Thus, we determine the BH masses using another method, before considering the total BH masses from stellar velocity dispersion. We can estimate the BH masses of central two black holes under the correlation  $M_{BH} - L_{5100\text{\AA}}$  found by Peterson et al. (2004),  $M_{BH1} \sim 6.5 \pm 1.1 \times 10^7 \text{ M}_\odot$  and  $M_{BH2} \sim 3.1 \pm 0.9 \times 10^7 \text{ M}_\odot$ , which is consistent with the mass ratio from the ratio of rotating velocity. The continuum luminosity of each black hole + BLRs system can be estimated from the luminosity of each broad component of  $\text{H}\alpha$  by equation 1, because of the small contributions from narrow components of  $\text{H}\alpha$ . Under the binary black hole system model, there is another parameter of projected angle of the orbital velocity to determine the structure of each BLR except the inclination angle of the orbit, thus we select the correlation between  $M_{BH} - L_{5100\text{\AA}}$  rather than eq 2. The total BH masses,  $9.6 \pm 2.0 \times 10^7 \text{ M}_\odot$ , determined from each broad  $\text{H}\alpha$  is similar to BH masses  $3.83_{-2.37}^{+4.44} \times 10^7 \text{ M}_\odot$  estimated from stellar velocity dispersion, which is consistent with the predicted result for merging galaxies by Kazantzidis et al. (2005).

Under the assumption of the BBH model, we accept the BH masses estimated from each broad  $\text{H}\alpha$  for each black hole. We can roughly estimate the separation of the central two black holes by:

$$\Omega^2 = \frac{G \times (M_{BH1} + M_{BH2})}{r^3} \quad (3a)$$

$$v_1 = \Omega \times \frac{M_{BH2}}{M_{BH1} + M_{BH2}} \times r \times \sin(i) \sin(\phi) \quad (3b)$$

where  $r$  is the separation between the central two black holes,  $i$  is the inclination angle of the rotating plane,  $\phi$  is the projected angle of the orbital velocity,  $\Omega$  is the angular speed,  $v_1$  is the observed rotating velocity in the line of sight of the clouds in BLRs including  $M_{BH1}$ . From the equations above, we can determine the upper limit value of the separation  $r$ :  $r < 40.8$  light-days, and the upper limit value of orbital period  $P$ :  $P < 59$  years. However, the size of each BLR can be determined by (Wang & Zhang 2003):

$$\log R_{BLRs} = (0.51 \pm 0.02) \log \left( \frac{L_{H\alpha}}{10^{44} \text{ erg} \cdot \text{s}^{-1}} \right) + (2.16 \pm 0.02) \text{ light-days} \quad (4)$$

The sizes of BLRs are about 45.1 light-days and 79.4

light-days for each BLR, which turns out larger than the maximum value of separation. In order to keep the completeness of each BLR, the sizes of the BLRs should not be larger than the separation of the two black holes. This poses some problem to the BBH model for SDSS J1130+0058. It has to be stressed, however, that the standard way to determine BLR sizes, may not be applicable for a BBH system.

Another model, the accretion disk model has been applied to explain the double-peaked  $H\alpha$ . Here, we select elliptical accretion disk model (Eracleous et al. 1995), because of the number of free parameters in the model which is less than those required by the circular accretion disk plus spiral arms model. The best fitted results with  $\chi^2 \sim 0.91$  are shown in Figure 7. The inner radius is about  $713 \pm 107R_G$ , outer radius is about  $6327 \pm 939R_G$ , eccentricity is about  $0.22 \pm 0.01$ , the inclination angle of the disk is about  $39 \pm 3^\circ$ . The slope of line emissivity is about  $\epsilon \propto r^{-1.58 \pm 0.11}$ . The local broadening velocity is about  $539 \pm 56 \text{ km} \cdot \text{s}^{-1}$ . According to the eccentricity, the period of the inner emission regions can be estimated as  $P_{pre} \sim 10.4 \frac{1+e}{(1-e)^{1.5}} M_6 r_3^{2.5} \sim 230 \text{ years}$ , where  $M_6$  is the central BH masses in unit of  $10^6 M_\odot$ ,  $r_3$  is the radius in unit of  $10^3 R_G$ .

More information, particularly about the variations of double-peaked broad  $H\alpha$  to determine the time scale and other characteristics of the variations of the lines is needed to verify whether the BBH model is valid for SDSS J1130+0058. From the theoretical side, a detailed model of the combined accretion disk emission from two accretion disks is yet to be developed.

### 3.4 Final Considerations

The only X-shaped radio source with apparent double-peaked broad emission lines, SDSS J1130+0058, is indeed an internally obscured AGN with standard continuum luminosity of a Seyfert 1 galaxy. The presence of internal dust may provide a convenient background for the backflow of material to produce X-shaped radio structures. But in this paper we found a smaller value of the reddening (and thus of the dust contents) than previously reported. We are not in the position to quantitatively support nor reject the backflow model, however a natural alternative is the BBH model. Objects with X-shaped extragalactic radio jets may be the signature of these binary systems.

A BBH system can also account for the observed dbp Balmer emission lines. Except for the problem with the sizes of the BLRs, the separation between the two black holes under the assumption of BBH model, is consistent with the theoretical expectation by Merritt & Ekers (2002), who found that the separation of the two black holes should be about 0.01 pc to 1 pc in a time shorter than 1 Gyr, if the coalescence rate of binary black holes is comparable to the galaxy merger rate. Under the BBH model, the separation of central black holes for SDSS J1130+0058 is about less than 0.04 pc. From the results of a single observation, we cannot rule out the BBH model. Moreover, the periods of BBH model and accretion disk model are very different, one is about 230 years and the other less than 59 years, so that long term observations are necessary to understand SDSS J1130+0058 better. Furthermore, the BBH model and accretion disk model will predict different variation patterns

of broad  $H\alpha$ . The BBH model leads to radial velocity of each peak varying in period. On the other hand, the accretion disk model cannot lead to the same result. Long term monitoring should provide more information to discriminate which model for SDSS J1130+0058 is favored.

There is another possibility within the BBH system scenario to explain the double-peaked broad emission lines and the X-shaped radio structures. The double-peaked broad emission lines are coming from the accretion disk of only one of the two central black holes. There is NO BLR around the other black hole. Otherwise, there would be three or more components of broad  $H\alpha$ . The X-shaped radio-structures are produced by the precession of the jet. The main effect of the existence of the second black hole is to produce the precession of the radio jet with respect to the accretion disk. In this case, the predicted behavior is that the center wavelength of broad  $H\alpha$  should vary in period, besides the variation of line profiles. Long term observations also can provide information to distinguish this model from the other two models.

### ACKNOWLEDGMENTS

ZXG gratefully acknowledges the postdoctoral scholarships offered by la Universidad Nacional Autonoma de Mexico (UNAM). D. D-H acknowledges support from grant IN100703 from DGAPA, UNAM. This paper has made use of the data from the SDSS projects. Funding for the creation and the distribution of the SDSS Archive has been provided by the Alfred P. Sloan Foundation, the Participating Institutions, the National Aeronautics and Space Administration, the National Science Foundation, the U.S. Department of Energy, the Japanese Monbukagakusho, and the Max Planck Society. The SDSS is managed by the Astrophysical Research Consortium (ARC) for the Participating Institutions. The Participating Institutions are The University of Chicago, Fermilab, the Institute for Advanced Study, the Japan Participation Group, The Johns Hopkins University, Los Alamos National Laboratory, the Max-Planck-Institute for Astronomy (MPIA), the Max-Planck-Institute for Astrophysics (MPA), New Mexico State University, Princeton University, the United States Naval Observatory, and the University of Washington.

### REFERENCES

- Abazajian K., et al., 2004, AJ, 128, 502
- Alexander P., Leahy J. P., 1987, MNRAS, 225, 1
- Antonucci R., Hurt T., Agol E., 1996, ApJ, 456, 25
- Bachev R., 1999, A&A, 348, 71
- Becker R. H., White R. L., Helfand D. J., ApJ, 1995, 450, 559
- Begelman M. C., Blandford R. D., Rees M. J., 1980, Nature, 287, 307
- Vanden Berk D. E., et al., 2001, AJ, 122, 549
- Blandford R. D., McKee C. F., 1982, ApJ, 255, 419
- Caproni A., Abraham Z., 2004a, ApJ, 602, 625
- Caproni A., Abraham Z., 2004b, MNRAS, 349, 1218
- Chen K. Y., Halpern J. P., 1989, ApJ, 344, 115
- Chen K. Y., Halpern J. P., Filippenko A. V., 1989, ApJ, 339, 742
- Chen K. Y., Halpern J. P., Titarchuk L. G., 1997, ApJ, 483, 194
- Chakrabarti S. K., Wiita P. J., 1994, ApJ, 434, 518
- Dennett-Thorpe J., Scheuer P. A. G., Laing R. A., Bridle A. H., Pooley G. G., Reich W., 2002, MNRAS, 330, 609

**Table 1.** Line Parameters of SDSS J1130+0058

Name	Center Wavelength Å	$\sigma$ km · s <sup>-2</sup>	flux 10 <sup>-17</sup> erg · s <sup>-1</sup> · cm <sup>-2</sup>
[NeV] $\lambda$ 3426Å	3426.7	125.3 $\pm$ 4.3	118.4 $\pm$ 3.8
[OII] $\lambda$ 3727Å	3728.8	175.6 $\pm$ 2.8	261.9 $\pm$ 4.1
[NeIII] $\lambda$ 3869Å	3869.9	114.2 $\pm$ 2.9	117.3 $\pm$ 2.9
[NeIII] $\lambda$ 3967Å	3969.4	141.3 $\pm$ 9.8	39.8 $\pm$ 2.6
H $\delta$	4103.2	103.3 $\pm$ 10.6	24.2 $\pm$ 2.3
H $\gamma$	4341.9	105.1 $\pm$ 5.9	53.4 $\pm$ 2.9
[OIII] $\lambda$ 4363Å	4364.9	116.4 $\pm$ 20.9	15.8 $\pm$ 2.7
HeII $\lambda$ 4686Å	4687.6	117.9 $\pm$ 6.4	54.6 $\pm$ 2.9
H $\beta$ (narrow)	4863.4	105.5 $\pm$ 2.1	139.8 $\pm$ 2.5
H $\beta$ (broad)			$f(H\alpha_{broad})/6.52$
[OIII] $\lambda$ 5007Å (normal)	5008.9	106.6 $\pm$ 0.4	1402.6 $\pm$ 11.5
[OIII] $\lambda$ 5007Å (broad)	5008.8	282.3 $\pm$ 17.1	150.6 $\pm$ 11.1
[NII] $\lambda$ 6583Å	6586.3	119.6 $\pm$ 1.8	289.7 $\pm$ 4.3
H $\alpha$ (narrow)	6565.6	112.5 $\pm$ 0.8	540.8 $\pm$ 3.8
H $\alpha$ (broad)	6563.0	2655.2 $\pm$ 22.1	2177.8 $\pm$ 27.9
[SII] $\lambda$ 6716Å	6719.3	122.5 $\pm$ 3.3	119.7 $\pm$ 2.8
[SII] $\lambda$ 6731Å	6733.8	129.6 $\pm$ 4.2	100.4 $\pm$ 2.7
double-gaussian components for broad H $\alpha$			
	6514.6	1283.8 $\pm$ 69.5	508.3 $\pm$ 79.7
	6590.8	2027.2 $\pm$ 84.6	1528.2 $\pm$ 91.8

$\sigma$  for each line is from the gaussian fitting.

Line parameters of broad H $\beta$  are estimated by the broad component of H $\alpha$ .

$f(H\alpha)$  represents the flux of broad H $\alpha$ .

The parameters of broad component of H $\alpha$  are from fitted results by one broad gaussian function for broad H $\alpha$ .

The parameters of [NII] $\lambda$ 6583Å are from fitted results by two gaussian functions for broad H $\alpha$ .

There are two components of [OIII] $\lambda$ 4959, 5007Å doublet, one normal with not much different line width as that of other narrow emission lines, one broad component with broader line width than that of other emission lines.

**Table 2.** Radio flux of SDSS J1130+0058

Name	ra	dec	int flux at 20cm mJy	offset arcminute
FIRST J113021.6+005820	11 30 21.6330	+00 58 20.000	152.94	0.075
FIRST J113020.9+005828	11 30 20.9480	+00 58 28.210	292.24	0.144
FIRST J113022.4+005820	11 30 22.4490	+00 58 20.740	77.58	0.262
FIRST J113020.1+005827	11 30 20.1810	+00 58 27.110	43.96	0.315

Eracleous M., Livio M., Halpern J. P., Storchi-Bergmann T., 1995, ApJ, 438, 610

Eracleous M., Halpern J. P., Gilbert A. M., Newman J. A., Filippenko A. V., 1997, ApJ, 490, 216

Ferrarese L., Merritt D., 2001, MNRAS, 320, L30

Gaskell C. M., 1983, Nature, 304, 212

Gebhardt K., et al., 2000, ApJ, 539, L13

Gilbert A. M., Eracleous M., Filippenko A. V., Halpern J. P., 1999, AAS, 194, 7302

Greene J. E., Ho L. C., 2005a, ApJ, 627, 721

Greene J. E., Ho L. C., 2005b, ApJ, 630, 122

Halpern J. P., Eracleous M., Filippenko A. V., Chen K. Y., 1996, ApJ, 464, 704

Hao L., et al., 2005, AJ, 129, 1783

Hartnoll S. A., Blackman E. G., 2000, MNRAS, 317, 880

Hartnoll S. A., Blackman E. G., 2002, MNRAS, 332, L1

Kaiser C. R., Dennett-Thorpe J., Alexander P., 1997, MNRAS, 292, 723

Kaiser C. R., Alexander P., 1997, MNRAS, 286, 215

Kaiser C. R., 2000, A&A, 362, 447

Karas V., Martocchia A., Subr L., 2001, PASJ, 53, 189

Kaspi S., Smith P. S., Netzer H., Maoz D., Jannuzi B. T., Giveon U., 2000, ApJ, 533, 631

Kaspi S., Maoz D., Netzer H., Peterson B. M., Vestergaard M., Jannuzi B. T., 2005, ApJ, 629, 61

Kazantzidis S., et al., 2005, ApJ, 623, L67

Kino M., Kawakatu N., 2005, MNRAS, 364, 659

Kormendy J., Gebhardt K., 2001, AIP Conf. Proc. 586, Relativistic Astrophysics, ed., C. Wheeler & H. Martel, 363

Leahy J. P., Williams A. G., 1984, MNRAS, 210, 929

Leahy J. P., Muxlow T. W. B., Stephens P. W., 1989, MNRAS, 239, 401

Le Borgne J. F., et al., 2003, A&A, 402, 433

Lehto H. J., Valtonen M. J., 1996, ApJ, 460, 207

Li C., Wang T. G., Zhou H. Y., Dong X. B., Cheng F. Z., 2005, AJ, 129, 669

Liu R., Pooley G., Riley J. M., 1992, MNRAS, 257, 545  
 Liu F. K., 2004, MNRAS, 347, 1357  
 Machalski J., Chyzy K. T., Stawarz L., Koziel D., 2006, A&A, astro-ph/0609680  
 Mahadevan R., 1997, ApJ, 477, 585  
 Mahadevan R., Quataert E., 1997, ApJ, 490, 605  
 Marziani P., Dultzin-Hacyan D., Sulentic J. W., 2006, in New Development in Black Hole Research, P. V. Kreitler (Editor), New York: Nova Science Publishers, pp. 123-183 (2006)  
 Merritt D., Ekers R. D., 2002, Science, 297, 1310  
 Narayan R., Yi I., Mahadevan R., 1995, NATURE, 374, 623  
 Narayan R., Yi I., Mahadevan R., 1996, A&AS, 120, 287  
 Nelson C. H., Whittle M., 1995, ApJS, 99, 67  
 Nelson C. H., Whittle M., 1996, ApJ, 465, 96  
 Nelson C. H., 2000, ApJ, 544, L91  
 Netzer H., Peterson B. M., 1997, in Astronomical Time Series, ed. Maoz D., Sternberg A. & Leibowitz E., 85  
 Onken C. A., Ferrarese L., Merritt D., Peterson B. M., Pogge, Richard W., Vestergaard M., Wandel A., 2004, ApJ, 615, 645  
 Ostorero L., Villata M., Raiteri C. M., A&A, 419, 913  
 Parma P., Murgia M., Morganti R., Capetti A., de Ruiter H. R., Fanti R., 1999, A&A, 344, 7  
 Peterson B. M., 1993, PASP, 105, 247  
 Peterson B. M., Wandel A., 1999, ApJ, 521, L95  
 Peterson B. M., et al., 2004, ApJ, 613, 682  
 Rix H. W., White S. D. M., 1992, MNRAS, 254, 389  
 Scott J. E., Kriss G. A., Brotherton M., Greene R., 2004, APJ, 615, 135  
 Shapovalova A. I., et al., 2001, A&A, 376, 775  
 Sillanpää A., Haarala S., Valtonen M. J., Sundelius B., Byrd G. G., 1988, ApJ, 325, 628  
 Sillanpää A., et al., 1996a, A&A, 315, L13  
 Sillanpää A., et al., 1996b, A&A, 305, L17  
 Storchi-Bergmann T., Baldwin J. A., Wilson A. S., 1993, ApJ, 410, L11  
 Storchi-Bergmann T., Eracleous M., Livio M., Wilson A. S., Filippenko A. V., Halpern J. P., 1995, ApJ, 443, 617  
 Storchi-Bergmann T., Eracleous M., Ruiz M. T., Livio M., Wilson A. S., Filippenko A. V., 1997, ApJ, 489, 87  
 Storchi-Bergmann T., et al., 2003, ApJ, 598, 956  
 Strateva I. V., et al., 2003, AJ, 126, 1720  
 Strauss M., et al., 2002, AJ, 124, 1810  
 Sulentic J. W., Zheng W., Calvani M., Marziani P., 1990, ApJ, 355, 15  
 Sulentic J. W., Zwitter T., Marziani P., Dultzin-Hacyan D., 2000, ApJ, 536, L5  
 Sulentic J. W., Repetto P., Stirpe G. M., Marziani P., Dultzin-Hacyan D., Calvani M., 2006, A&A in press, astro-ph/0606309  
 Tremaine S., et al., 2002, ApJ, 574, 740  
 Tudose V., Fender R. P., Kaiser C. R., Tzioumis A. K., van der Klis M., Spencer R., 2006, MNRAS, 372, 417  
 Valtonen M. J., et al., 2006a, ApJ, 643, 9  
 Valtonen M. J., et al., 2006b, ApJ, 646, 36  
 Vicente L., Charlot P., Sol H., 1996, A&A, 312, 727  
 Wang T. G., Zhou H. Y., Dong X. B., 2003, AJ, 126, 113  
 Wang T. G., Zhang X. G., 2003, MNRAS, 340, 793  
 Worrall D. M., Birkinshaw M., Cameron R. A., 1995, ApJ, 449, 93  
 York D. G., et al., 2000, AJ, 120, 1579  
 Zhang Xue-Guang, Dultzin-Hacyan D., Wang Ting-Gui, 2006, being prepared  
 Zhang Xue-Guang, Dultzin-Hacyan D., Wang Ting-Gui, 2007, Rev. Mex. A&A, 43, 1, astro-ph/0610432  
 Zheng W., O'Brien P. T., 1990, ApJ, 353, 433

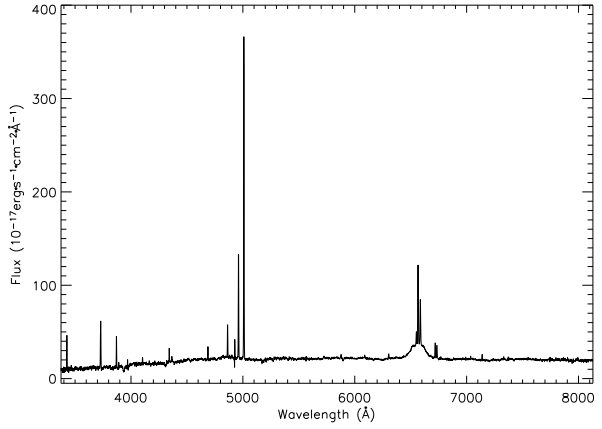


Figure 1. The observed spectrum of SDSS J1130+0058.

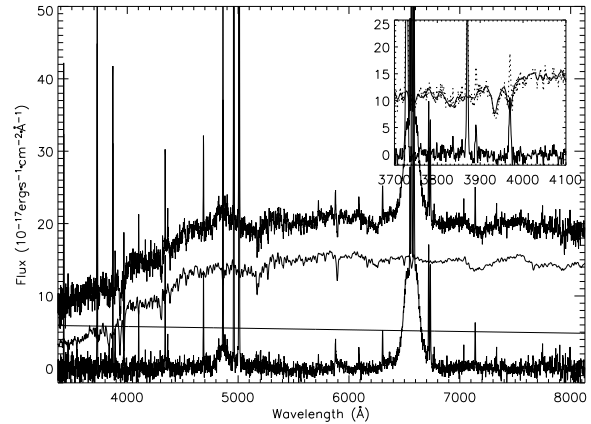
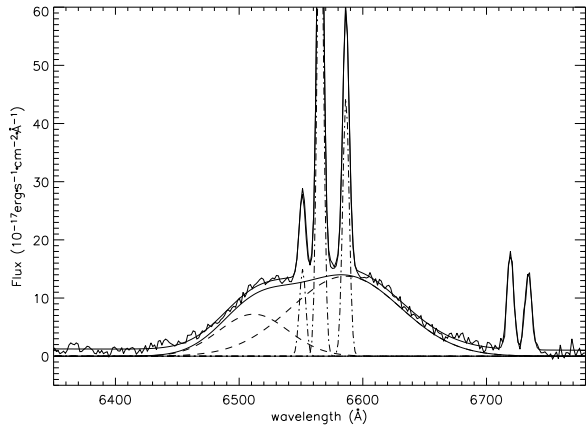
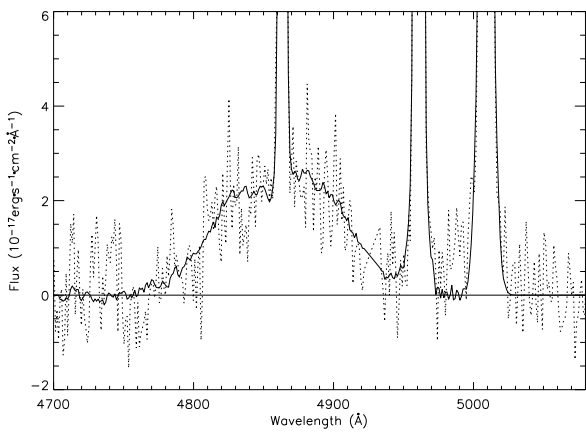


Figure 2. The spectrum of SDSS J1130+0058. The upper one is the observed spectrum. The middle two are the components of stellar lights and the power continuum. The bottom one is the line spectrum after the subtraction of stellar lights and continuum. The detailed results for CaIIλ3934, 3974Å are shown in top right corner, the dotted line represents the observed spectrum, solid lines is the best fitted results and line spectrum in this region.



**Figure 3.** The best fitted results for H $\alpha$ . Thin solid line represents the line spectrum. Tick solid line is the best fitted results. The dashed lines are the two broad components for broad H $\alpha$ . Dot-dashed lines are the narrow emission lines. The fitted broad H $\alpha$  is shown as solid line under the observed line spectrum.



**Figure 4.** The best fitted results for H $\beta$ . Dotted line represents the line spectrum. Solid line is the best fitted results by scaling of the observed broad H $\alpha$ .

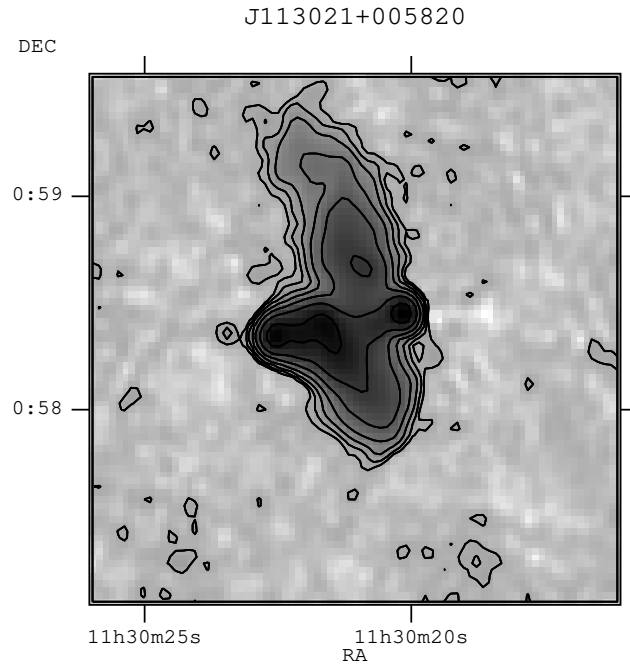


**Figure 5.** The radio image at 20 cm of SDSS J1130+0058.

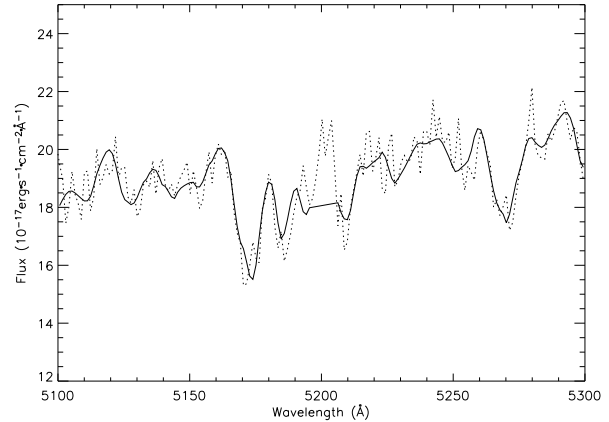


**Figure 6.** The fitted results for stellar features near MgIb $\lambda$ 5175 $\text{\AA}$ . The dotted line represents the observed spectrum. The solid line represents the best fitted results with  $\chi^2 \sim 0.97$  by eight eigenspectra from spectra of stars.

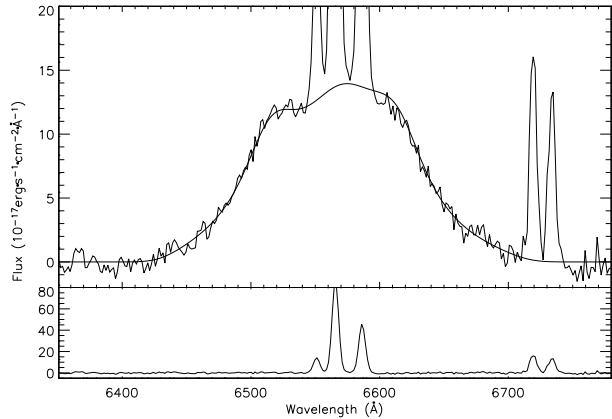


**Figure 7.** The best fitted results for double-peaked broad H $\alpha$  by elliptical accretion disk model. The dotted line represents the line spectrum, solid line is the best fitted results for broad H $\alpha$ . The lower pannel shows the line spectrum after the subtraction of broad component of H $\alpha$ .